Targeted Nanoparticles for Cardiovascular Molecular Imaging

Gustav J. Strijkers

Abstract Molecular imaging is aimed at noninvasive visualization of fundamental (disease) biomarkers in living organisms. Molecular imaging holds great promise in facilitating patient-specific disease diagnosis, treatment planning, monitoring of local drug delivery, and early evaluation of therapy. This paper reviews recent major accomplishments in the field of molecular imaging of cardiovascular disease, with particular focus on the use of nanoparticles as signal beacons for target-specific imaging.

Keywords Molecular imaging · MRI · CT · Nanoparticles · Cardiovascular disease · Atherosclerosis · Coronary heart disease · Myocardial infarction

Introduction

The cardiovascular system is responsible for the distribution of oxygen, nutrients, cells, and signaling molecules in the human body, and the removal of waste products to maintain cellular homeostasis and fight disease. The cardiovascular system consists of the blood distribution network (the heart and the blood vessels), but in a broader view the lymphatic system can also be included. With every beat, the heart pumps blood through the pulmonary circulation to pick up oxygen and remove gaseous waste products, and into the systemic circulation to provide oxygen and pick up and deliver nutrients to the body. The heart is the strongest muscle in the body and an apparently tireless pump, typically beating 60–70 times per minute and accumulating more than 2 billion heartbeats over a lifespan of 70 years. The cardiovascular system is of primary importance to maintaining a healthy condition. Unfortunately however, the heart and blood vessels are not immune to disease. Both are susceptible to breakdown and attacks from various diseases, which are collectively referred to as cardiovascular disease (CVD).

There exist a large number of diseases that affect the cardiovascular system at various levels, leading to disability and death. Those which occur most frequently include rheumatic heart disease, congenital heart disease, aneurisms, peripheral artery disease, thrombosis, pulmonary embolism, stroke, and coronary heart disease (CHD) [1]. Taken together, an estimated 17.3 million people worldwide died from CVD in 2008—a number that is expected to increase to more than 23 million in 2030. More people die annually of CVD than from any other cause. Of all CVDs, stroke and coronary artery disease account for more than 70 % of all deaths. Risk factors for CVD are well known and involve smoking, obesity, diabetes, hyperlipidemia, physical inactivity, and hypertension. Nevertheless, it is unrealistic to expect that the CVD epidemic can be halted by prevention, raising public awareness and changes in lifestyle alone. Hence, there is great need for new treatment strategies and tools to determine the condition of the individual patient at risk for or suffering from CVD, in order to predict and improve clinical outcome and to accurately monitor and screen response to new therapies.

Molecular imaging holds the promise to revolutionize the understanding of the etiology of CVD, thereby profoundly impacting future clinical CVD care [2–5]. The use of targeted molecular imaging probes enables the identification of key pathophysiological events, including

G. J. Strijkers (✉)
Biomedical NMR, Department of Biomedical Engineering,
Eindhoven University of Technology, P.O. Box 513,
5600 MB Eindhoven, The Netherlands
e-mail: g.j.strijkers@tue.nl

necrosis, inflammation, thrombosis, necrosis, apoptosis, remodeling, and revascularization. Novel therapies for CVD, such as those based on cellular therapy and using innovative therapeutic compounds may greatly benefit from the insights obtained by molecular imaging. In the future, the use of nanoparticles may enable combined (targeted) imaging and drug delivery tailored to the patient's specific CVD molecular fingerprint.

In this review, recent promising developments in the use of nanoparticles for molecular imaging of CVD are highlighted and discussed. For reason of focus, this review mainly covers the molecular imaging of CHD.

Coronary Heart Disease

Coronary heart disease can be defined as diseases of the blood vessels supplying the heart muscle and resulting clinical complications. Most coronary circulation problems are related to the formation of atherosclerotic plaques in the major branches of the coronary arteries [6–8]. Although many aspects of the etiology of atherosclerosis remain unknown, the formation of an atherosclerotic plaque is generally accepted to be an inflammatory response to buildup of low-density lipoprotein (LDL) in the vessel wall. This early plaque is referred to as a fatty-streak. LDL uptake in the sub-intima is followed by LDL oxidation by free radicals, originating from myeloperoxidase (MPO) produced by macrophages and neutrophils. The oxidized-LDL in turn triggers an aggravated inflammatory reaction and increased endothelial dysfunction, leading to intensified recruitment and activation of cells of the immune system. Macrophages absorb the oxidized-LDL to become foam cells, which eventually rupture and thereby gradually accumulate lipids in the plaque core. Recruited macrophages also release enzymes, such as matrix metalloproteinase (MMP), that degrade the extracellular matrix and lead to necrosis and apoptosis of endothelial cells, smooth muscle cells and macrophages. Dying cells deposit calcium leading to extracellular calcification of the plaque. New fragile blood vessels may be formed in the plaque, which are leaky and lead to intraplaque hemorrhage. Eventually, this slow-progressing cascade of self-sustaining events may lead to artery occlusion or to vulnerable plaque rupture, causing an acute thrombotic event. In other cases, the process may linger over a lifetime and the plaque may stay clinically silent. Clinical risk assessment by prediction of plaque vulnerability using noninvasive (molecular) imaging technology remains a great, unsolved challenge.

Clinical complications resulting from atherosclerosis in the coronary artery tree include angina pectoris, as a consequence of a partly obstructed coronary artery, and myocardial infarction due to full occlusion of a coronary artery after a thrombotic event. The molecular processes following myocardial infarction have many parallels with atherosclerotic disease [9, 10]. Cell death proceeds principally via apoptosis in the early hours after infarction and through necrosis thereafter. Reperfusion of the affected coronary artery by aggressive thrombolytic therapy to dissolve the occlusive cloth may limit the amount of necrosis but causes additional apoptosis and inflammation. Leukocytes, carried to the infarct by the blood, release a number of inflammatory factors as well as free radicals in response to tissue damage. Later, granulation tissue is produced by fibroblasts and contractile myofibroblasts, providing new tensile strength to the infarct area.

Imaging Inflammation in Cardiovascular Disease

Inflammation plays a key role in CHD and is considered an important sign of atherosclerotic plaque vulnerability. In recent years, a number of targeted agents have been employed to visualize plaque inflammation using various imaging modalities. The nuclear techniques (e.g. PET) have superior sensitivity for the detection of low concentrations of tracer material. Several years ago, it was found that FDG uptake in plaques correlates with macrophage content and is considerably higher in inflamed plaques than in control vessels [11–13]. FDG signal in plaques responds to anti-inflammatory treatment [14]. PET-FDG may therefore be an attractive imaging modality to study and through which to evaluate novel therapeutics aimed at silencing plaque inflammation and reducing rupture risk. On the other hand, FDG may not be specific to plaque inflammation alone since other factors, such as hypoxia and neovascularization, may increase uptake as well. Also, PET-FDG of coronary vessels is problematic due to the close proximity of the myocardium, which avidly takes up FDG. Other PET tracers for imaging inflammation are therefore under development [15].

The limited spatial resolution of PET hampers accurate localization of signals in small plaques in moving vessels. For this purpose, magnetic resonance imaging (MRI) and computed tomography (CT) have distinct advantages. MRI combines high spatial and temporal resolution with a variety of readouts of plaque and vessel morphology [16]. CT angiography is considered the most clinically robust and accurate method for grading coronary artery stenosis and determining plaque calcification [17]. On the downside, MRI and CT have limited sensitivity for the detection of molecular tracers and therefore require a suitable amplification strategy.

One of the first type of nanoparticles applied to study plaque inflammation by MRI were the iron oxide nanoparticles, including superparamagnetic iron oxide (SPIO)

and ultrasmall superparamagnetic iron oxide particles (USPIO). Following the finding that carbohydrate-coated iron oxide nanoparticles are rapidly phagocytosed by macrophages and accumulate in spleen, liver, bone marrow and lymph nodes, thus enabling MR imaging of macrophage activity in these organs, the particles were also found to specifically accumulate in plaque resident macrophages. In a rabbit model of atherosclerosis, Ruehm et al. [18] demonstrated specific signal loss in T2*-weighted images of the aorta originating from USPIO accumulation in plaque macrophages. In patients originally scheduled to receive MRI for staging lymph node metastases, accumulation of SPIOs was observed as pronounced signal loss in T2*-weighted images in aortic and arterial wall segments [19]. Kooi et al. [20] demonstrated significant signal loss in T2*-weighted images of human carotid artery plaques 24 h after injection of USPIOs. After surgical resection of the lesion, histological and electron microscopy confirmed the presence of the USPIOs in the plaque primarily located in macrophages. In patients, aggressive lipid-lowering therapy over a 3-month period resulted in significant reduction of USPIO-detected inflammation, demonstrating that inflammation imaging by MRI could develop into a useful clinical tool to evaluate anti-inflammatory treatment [21]. A possible complication for the use of these types of particles in imaging plaque inflammation is that accumulation of iron oxides in perivascular lymph nodes may lead to false positive findings depending on the choice of imaging sequence and image resolution [22].

Iron oxide nanoparticles have also been extensively investigated to assess inflammation in the heart. Kanno et al. [23] used USPIOs to study acute allograft rejection in rat after heart and lung transplantation. In rats that received a syngeneic transplant, injection of USPIOs 6 days after surgery did not result in signal changes on gradient-echo MRI at day 7. In rats that received an allotransplant leading to acute rejection, significant signal losses were observed, which could be attributed to USPIO-laden infiltrating macrophages. The response could be modulated by anti-inflammatory treatment. Sosnovik et al. [24] used iron oxides to visualize macrophages in the infarcted mouse myocardium. The uptake of the iron oxides by macrophages infiltrating the infarcted myocardium was confirmed by fluorescence microscopy and immunohistochemistry. In mice, injection of micron-sized particles of iron oxide (MPIO) 7 days before infarct surgery resulted in a gradual signal decrease over time in T2*-weighted images of the infarcts [25]. Signal loss could be attributed to the influx of pre-labeled macrophages that were recruited to the infarct.

The iron oxides are under investigation for tracking inflammatory cells in humans after recent myocardial infarction. Figure 1 highlights a recent study, in which patients with acute myocardial infarction were imaged at baseline and at 24 and 48 h after injection of USPIOs (ferumoxytol; AMAG Pharmaceuticals, Lexington, MA) [26••]. Injection of USPIO in healthy subjects did not result in R2* (=1/T2*) enhancement in the myocardium, and without injection of contrast agent the R2* values in patients with recent myocardial infarction were stable at these time points (Fig. 1a–c). Application of the USPIOs gave rise to a strong increase in R2* in the infarcts, peaking at 24 h after injection (Fig. 1d, e). Although no histological validations were performed in this study, these observations together with previous knowledge obtained from animal studies strongly suggest that iron oxide-laden macrophages infiltrated the infarcts and that the strong R2* increase therefore indicated the inflammatory response after infarction. Interestingly, an R2* increase was also seen in remote myocardium, although to a lesser extent, indicating post-infarct inflammatory cell infiltration in remote myocardium as well. This technique may find clinical application in the assessment inflammatory response after myocardial infarction and in the evaluation of treatment aimed at controlling the inflammatory response. It could also be of interest for other inflammatory diseases of the heart.

A potential drawback of the use of iron oxides is that T2*-weighted MRI and its associated R2* mapping is artifact prone. Particularly in the assessment of small atherosclerotic plaques and to a lesser degree in the heart, partial volume effects, susceptibility mismatch, blood flow and movement artifacts may be mistaken for nanoparticle-induced signal loss. Several alternative approaches therefore were developed. Nanoparticles suitable as a T1 lowering agent allow for the use of fast T1-weighted MRI methods and inversion recovery imaging techniques resulting in a positive signal change, which can be attributed less ambiguously to areas of nanoparticles accumulation.

In one such approach, Naresh et al. [27, 28] employed Gd-labeled liposomes for targeting macrophages in a mouse model of myocardial infarction. Figure 2 shows three inversion recovery T1-weighted MR images (Fig. 2a–c) of a mouse heart at day 2 and 4 after induction of myocardial infarction. At day 2 (Fig. 2a), traditional late gadolinium enhancement (LGE) using Gd-DTPA contrast agent confirmed the presence of a large infarct. After injection of Gd-liposomes at day 2 (Fig. 2b), T1 contrast in the myocardium was not immediately observed. At day 4 (Fig. 2c), however, a bright signal was apparent particularly in the infarct core, which was attributed to the presence of macrophages labeled with Gd-liposomes. In a slightly different study setup, the Gd-liposomes were injected 2 days before the infarct surgery to pre-label monocytes. Serial measurements of the difference in the longitudinal relaxation rate R1 (=1/T1) of the myocardium
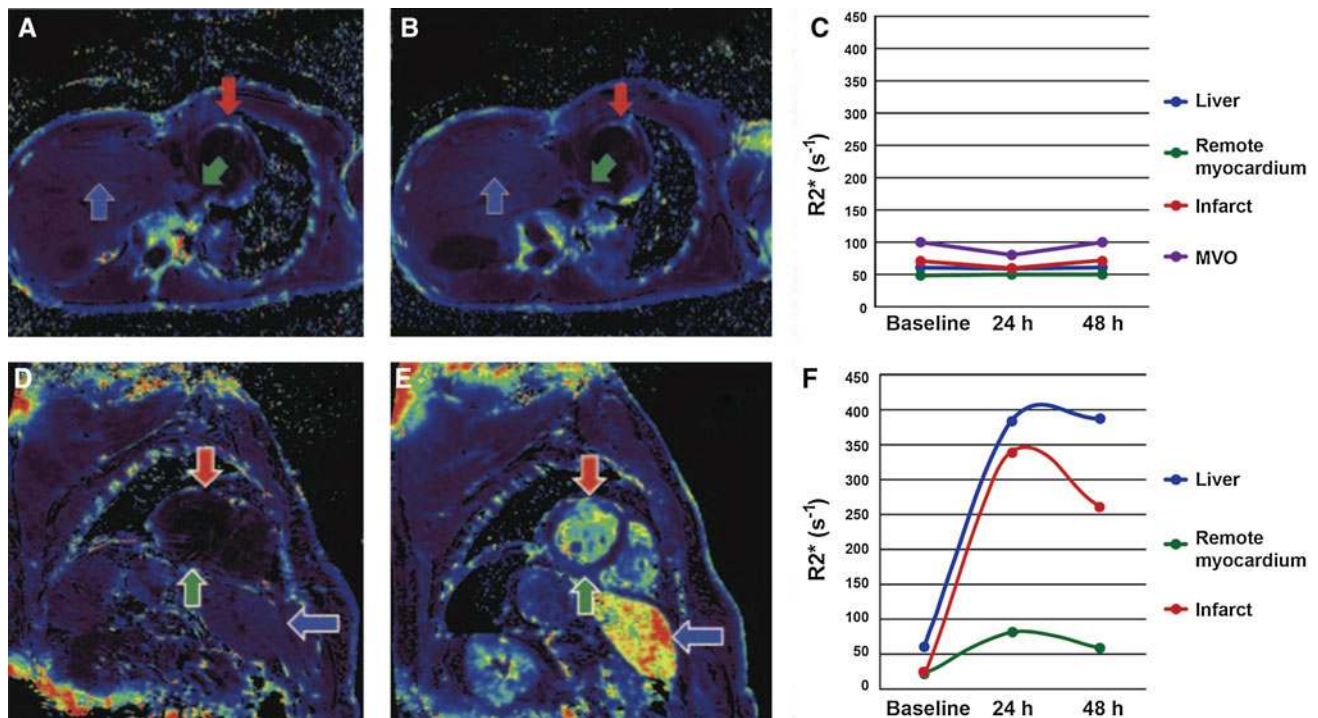
Fig. 1 Use of iron oxide nanoparticles to study the inflammatory response after myocardial infarction in humans. R2* maps of the hearts of patients with recent myocardial infarction at **a**, **d** baseline and **b**, **e** 24 h after **a**, **b** no infusion or **d**, **e** infusion of iron oxides. **c** R2* values in the heart without injection remained stable, whereas **f** infusion of iron oxides resulted in highly elevated R2* values in the infarct and to a lesser extent in the remote myocardium. R2* mapping after infusion of iron oxide nanoparticles therefore shows great promise for clinical MR imaging of inflammation in the heart. *Reproduced from* [26••], *with permission*

between non-injected and injected mice (Fig. 2d) displayed a significant increase that peaked at day 4 after infarct induction, revealing the time course of macrophage infiltration into the infarct zone. A small increase in R1 was also observed in the remote zone, which indicates inflammatory cell infiltration in this region in agreement with observations using iron oxides described above.

Although T1-weighted imaging is less prone to artifacts than T2*-weighted imaging, the use of Gd-labeled nanoparticles is not without complications. First of all, affinity of the Gd-labeled liposomes for inflammatory cells proves highly dependent upon the (surface) composition of the particles. Paulis et al. [29] and Geelen et al. [30•] have recently shown that pegylated Gd-liposomes and smaller Gd-micelles readily accumulate in the myocardium of mice with an infarction induced by either permanent or transient occlusion of a coronary artery. In both studies, only minor association of nanoparticles with inflammatory cells was observed, indicating that the contrast enhancement in the infarcts observed on T1-weighted imaging reported on the perfusion status of the myocardium and vascular hyperpermeability rather than on the presence of inflammatory cells. Previously, such passive accumulation of Gd-labeled liposomes and micelles was also observed in mouse atherosclerotic plaques [31, 32]. Passive accumulation of nanoparticles through damaged vasculature in diseased

tissues leads to background signal that reduces the contrast to background ratio for imaging with targeted nanoparticles. Passive accumulation must be considered not only for the Gd-containing liposomes, but also for other types of nanoparticles such as the iron oxides. On the other side, massive accumulation of nanoparticles in the myocardium opens new opportunities for delivering large payloads of therapeutics [29, 30•]. Secondly, T1 and contrast changes induced by Gd-containing nanoparticles may be less appropriate for absolute quantification purposes, since several studies have shown that the relaxivity of the nanoparticles is strongly reduced upon internalization of the nanoparticles in cells [33–37].

A powerful alternative to iron oxide and Gd-labeled nanoparticles for imaging inflammation are 19F-containing nanoparticles. The 19F atom can be imaged directly with 19F-MRI and since the human body contains very little native fluorine, the nanoparticles can be imaged in an MRI silent background enabling unambiguous identification of inflammatory 'hot spots'. A recent example of such an approach applied to the heart is illustrated in Fig. 3 [38, 39••]. Here, perfluorocarbon (PFC) nanoparticles containing a high payload of 19F atoms were injected in mice shortly after infarct surgery. Flow cytometry revealed that approximately 50 % of the blood monocytes and macrophages were labeled with PFC 2 h after injection. Labeled
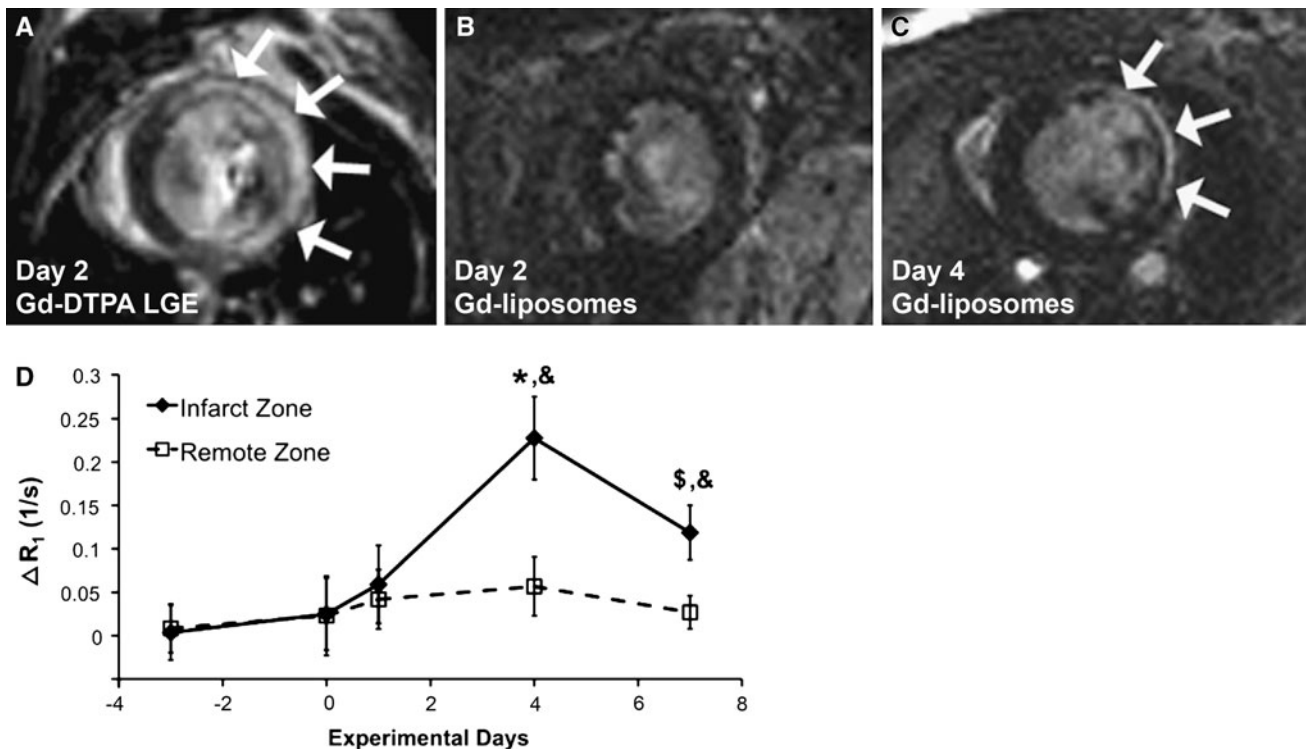
Fig. 2 Application of Gd-liposomes for imaging of inflammation after myocardial infarction in mice. Inversion recovery MR image of an infarcted mouse heart **a** at *day 2* using Gd-DTPA late gadolinium enhancement (LGE) to depict location and size of the infarction, **b** at *day 2* after injection of Gd-labeled liposomes, and **c** at *day 4*, 2 days after injection of the liposomes. Enhancement of the infarct core resulted from liposome labeled macrophages that infiltrated in the infarct. **d** R1 measurements in infarct zone and remote zone. Gd-liposome accumulation in the infarcts reached maximal levels on day 4 after myocardial infarction. *Reproduced from* [27, 28], *with permission*

inflammatory cells subsequently infiltrated the infarct myocardium, where they could be imaged with 19F-MRI (Fig. 3). Signal intensities from the 19F-density MRI sequence are proportional to the amount of 19F and there is no background signal other than noise, and therefore the 19F-MR images report on the severity of the inflammation. The approach may therefore be applicable to monitoring the efficacy of therapeutic interventions. PFCs are nontoxic and biochemically inert and some PFC-emulsions already have been clinically applied as an artificial blood substitute [40]. We may therefore expect a rapid clinical translation of this approach to inflammation imaging.

Various Targets

To improve specificity, nanoparticles may be equipped with moieties that target inflammation or other processes involved in the CVD pathways. Maiseyeu et al. [41] reported on the use of phosophatidylserine-containing liposomes for specific targeting of macrophages in atherosclerotic plaque. Phosphatidylserine (PS) is known to promote phagocytosis by inflammatory cells. In an ApoE−/− mouse model of atherosclerosis, injection of Gd- and PS-containing liposomes

resulted in distinct signal enhancement in T1-weighted images of plaques in the aorta (Fig. 4). Liposomes in the plaques colocalized with macrophages. In a similar approach, Geelen et al. [42, 43] developed a Gd-containing liposome with PS for imaging of myocardial infarction and showed that liposomes with 6 mol % PS were maximally internalized by murine macrophages.

Nanoparticles may be equipped with peptides, proteins or antibodies for targeting monocytes/macrophages [22, 44–49]. However, use of such ligands may be less suitable for clinical translation because of costs, toxicity and problems with immunogenicity. Nevertheless, the use of recognition ligands opens the opportunities for molecular MR imaging of other components of the coronary artery disease pathways, including dysfunctional endothelium, enzymatic activity, cell death, neovascularization, thrombosis, and extracellular matrix production or breakdown.

Targeted nanoparticles for MR imaging of inflamed endothelium were developed and applied in proof of concept studies in murine models of atherosclerosis [50–54], stroke [55–58], renal injury [59] and myocardial infarction [60, 61]. MMP expression was imaged using a small peptide with affinity for MMPs covalently bound to a small Gd-chelate in atherosclerosis [62–64]. Te Boekhorst et al.
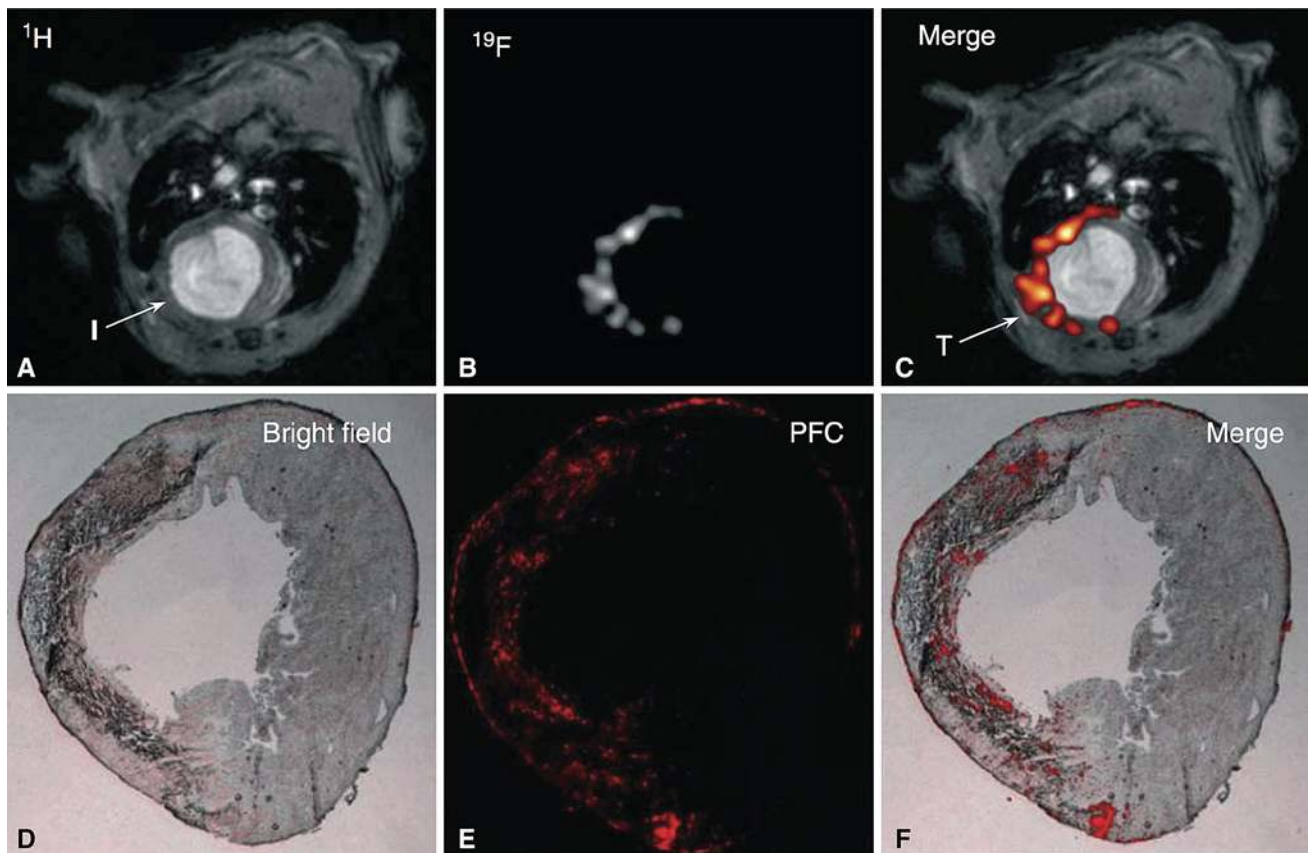
Fig. 3 Imaging of perfluorocarbon (PFC) emulsions after myocardial infarction in mice. Injection of the PFCs was done 2 h after infarct surgery. MRI was performed after 4 days. **a** 1H-MRI of the mouse heart for anatomical reference. **b** 19F-MRI of the same slice and **c** a 19F/1H overlay image showing 'hot spots' in the infarct (indicated by *I*) and in the wound where the thorax was opened for surgery (indicated by *T*). **d** Bright-field microscopy confirmed the location of the infarct. **e** PFC rhodamine fluorescence and **f** image overlay revealed colocalization of PFCs with monocytes and macrophages in the infarct. *Reproduced from* [38, 39••], *with permission*

[65] developed Gd-containing micelles targeted towards neutrophil gelatinase-associated lipocalin-2 (NGAL), a protein that is associated with adverse cardiovascular events in patients after carotid endarterectomy. A small Gd-based contrast agent (Gd-MPO) was developed to image the enzyme MPO, excreted by monocytes, macrophages and neutrophils in inflamed tissues [66, 67]. The enzymatic activity of MPO leads to polymerization of Gd-MPO, which due to its increased size, gets subsequently trapped in the tissue. The Gd-MPO probe was validated in animal models of inflammation in atherosclerosis [68] and myocardial infarction [69•]. A number of targeted Gd- and iron oxide-based nanoparticles were developed for imaging apoptotic cell death in atherosclerotic plaque and infarcted myocardium [70–78]. Necrosis could be imaged with MRI using a Gd-based contrast agent that binds to exposed DNA fragments after necrotic cell death [79, 80]. The role of neovascularization in atherosclerosis was extensively studied using Gd- and 19F-containing nanoparticles [81–86]. Various products in the coagulation cascade, including fibrin, have been exploited for molecular MRI of thrombus using targeted Gd-chelates and nanoparticles [87–95]. Fibrosis plays a major role in atherosclerosis and a thick fibrous cap shielding the blood from thrombogenic material is considered to be a sign of a stable plaque. Excessive collagen formation in myocardial disease reduces cardiac function and may induce cardiac arrhythmia. Various targeted approaches for imaging fibrosis with MRI have been described in literature, using collagen- and elastin-binding peptides [96–100••] and proteins [101–104].

Molecular MRI using nanoparticles may develop into a powerful asset for studying CVD, particularly when combined with the more traditional functional and physiological MRI methods that have long been available for assessing the heart and blood vessels. There is certainly no lack of new ideas and many new clever concepts for molecular imaging of CVD beyond the strategies outlined in this review are continuously being developed. Unfortunately, many of the new concepts have not survived beyond proof of principle studies in (mostly murine) animal models of CVD. Imaging studies in small animal models of disease are certainly valuable for gaining increased
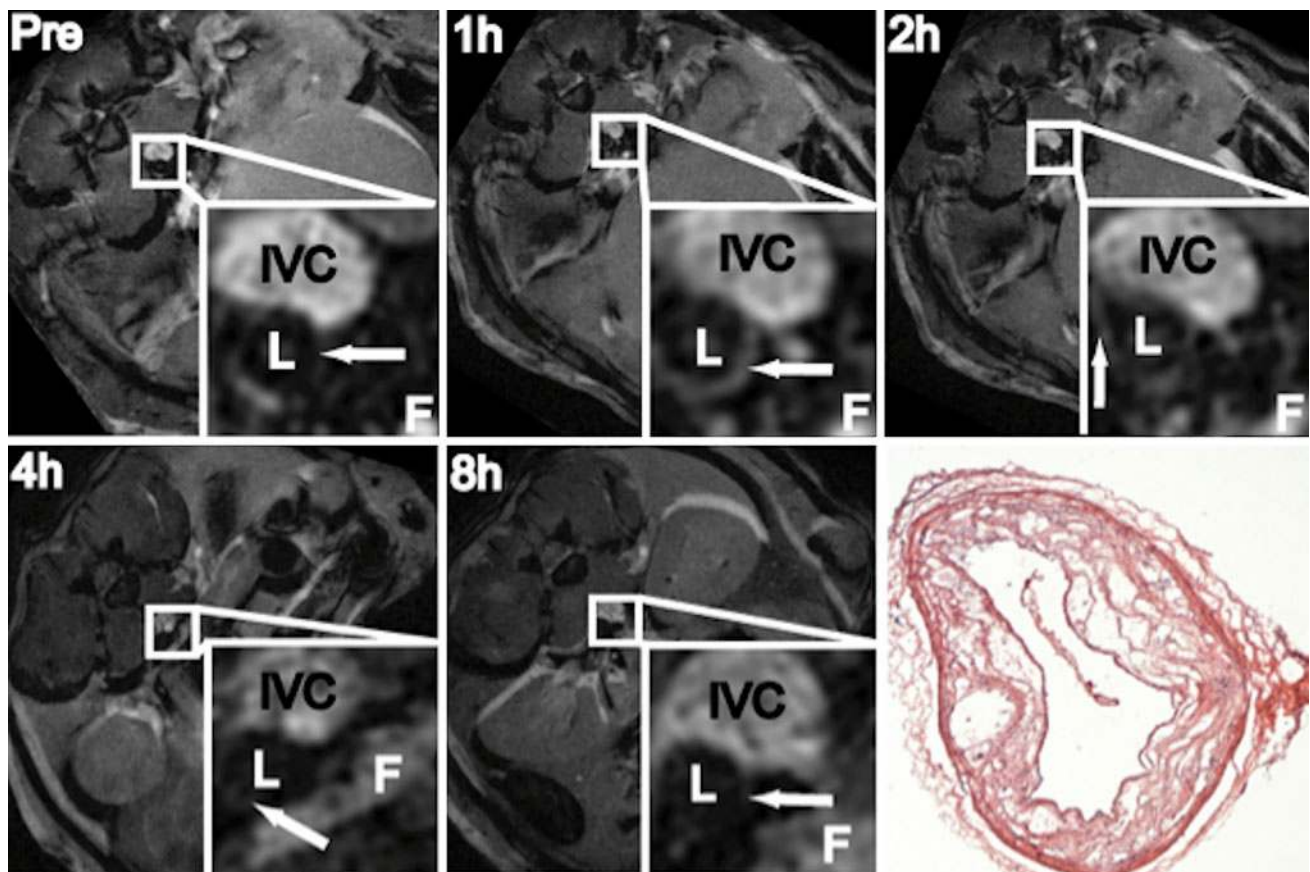
Fig. 4 Liposomes containing Gd and phosphatidylserine (PS) for specific recognition by macrophages in mouse atherosclerotic plaque. After injection of PS-containing liposomes, specific signal enhancement could be observed in plaques in the aorta of ApoE−/− mice (*white arrows* in the *inset images*). Maximum contrast was observed 2 h after injection. *IVC* inferior vena cava, *L* lumen, *F* abdominal fat. The *bottom-right* image is a histological section stained with Hematoxylin-Eosin. *Reproduced from* [41], *with permission*

understanding in disease mechanisms and for developing new treatment strategies with emerging therapeutics. Nevertheless, ultimately the goal is to translate successful concepts to clinical research and routine patient care. The reasons for lacking or slow translation towards human application are manifold. First of all, there are practical hurdles considering costs and industrial return on investment for a widespread use of targeted nanoparticles in diagnostic routine. Also, there are serious concerns about the safe application of nanotechnology in humans [105, 106]. The use of proteins, peptides or antibodies may lead to immunogenicity problems. Additionally, there are complications concerning slow blood clearance kinetics of certain nanoparticles and unfavorable clearance pathways via the liver and spleen, which may lead to accumulation of metals and other nanoparticle material in the body with uncertain and yet unknown long-term health consequences. To address some of these issues, interest has grown in the use of natural nanoparticles such as viruses [107], (apo-)ferritin [108–110] and lipoproteins [111], suitably modified for molecular imaging purposes. The use of modified high-density-lipoprotein (HDL) nanoparticles is specifically relevant for CVD and seems particularly promising, and therefore will be discussed in more detail in the following section.

HDL Nanoparticles

HDL is composed of a hydrophobic core of mainly tri-glycerides and cholesterol esters surrounded by a phospholipid monolayer. The enclosing shell contains the apolipoprotein A-1 (apoA-I). HDL transports cholesterol in the body and enables reverse cholesterol transport from atherosclerotic plaque. HDL has anti-thrombotic properties and modulates plaque inflammation and oxidation [112]. The HDL particle therefore plays a key role in plaque etiology, and application of HDL can serve both imaging [113] as well as therapeutic purposes [114]. HDL can be modified to include contrast-generating material. Incorporation of Gd in the phospholipid shell facilitates MR imaging of atherosclerotic plaque [115–117]. Various versions of modified HDL particles were designed that enabled imaging not only with MRI, but also with CT and

Fig. 5 Ex vivo spectral CT images of the thorax and abdomen of an ApoE−/− mouse with atherosclerotic plaque in the abdominal aorta. Mice were injected with Au-HDL nanoparticles and traditional iodinated CT contrast, 24 h prior to and just before imaging, respectively. **a** Conventional CT image in sagittal orientation. **b** Spectral CT image of gold. **c** Overlay showing Au-HDL accumulation in the aortic plaques. **d** Conventional CT image in transverse orientation. **e** Overlay image of gold (*yellow*), iodine (*red*; vasculature), photoelectric effect (*blue-white*; bone/calcium-rich), and Compton effect (*gray*; soft tissue). *Reproduced from* [119••], *with permission* (Color figure online)
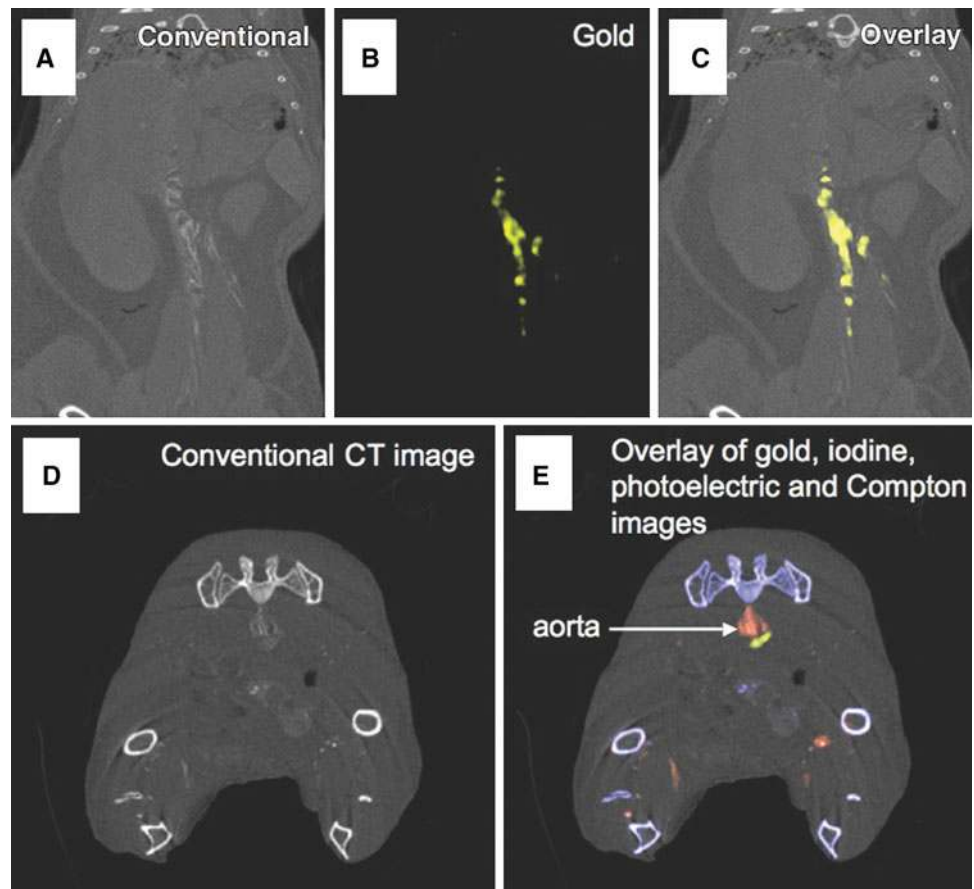
optical imaging [113]. Moreover, the modified HDL particles were used to study lipoprotein–lipoprotein interactions [118].

Gold containing HDL (Au-HDL) nanoparticles were employed to visualize atherosclerotic plaque in mice using spectral CT imaging [119••]. Spectral CT enables identification of materials by taking advantage of the polychromatic nature of the X-ray spectrum when creating CT images. Atherosclerotic plaques in the abdominal aorta of ApoE−/− mice were studied (Fig. 5). Au-HDL was injected 24 h prior to imaging. Shortly before imaging, a conventional iodine-based CT contrast agent was also injected for visualization of the vasculature. As shown in Fig. 5, spectral CT images enabled differentiation of the X-ray spectrum into gold, iodine, tissue and calcium (bone). High attenuation of X-rays in the atherosclerotic plaque could be attributed to accumulation of Au-HDL, which was found to largely colocalize with macrophages. This study demonstrates that molecular imaging with CT and biologically relevant nanoparticles is possible. A limitation to the study was that CT scanning times were impractically long because of low detector efficiency. Imaging therefore had to be performed ex vivo. However, this limitation may be overcome by improved detector technology.

Recently, a collagen-specific peptide conjugated HDL nanoparticle was developed and used for MR imaging of compositional changes in atherosclerotic plaque regression [100••]. Pre-clinical studies were performed in the so-called Reversa mouse model, in which plaque formation can be reversed by switching from a high-fat diet to normal chow, resulting in a decrease in the number of plaque macrophages and an increase in plaque collagen content [120]. HDL collagen specificity was introduced by attaching a collagen-specific peptide (EP-3553). HDL conjugated to non-specific peptide (EP-3612) and non-conjugated HDL were used as a control. Figure 6 summarizes the main findings of the study. At day 0, high macrophage and low collagen content in the plaques resulted in significant enhancement in T1-weighted MRI of the aortic plaques after injection of non-specific controls, whereas only minor signal increase was observed with collagen-specific HDL. After 28 days of plaque regression in the Reversa mice, enhancement was primarily observed after injection of collagen-specific HDL, indicating increased collagen and reduced macrophage content in the stabilized plaques. This study elegantly showed that the HDL nanoparticles can be used for in vivo MRI monitoring of plaque composition and changes therein after treatment.
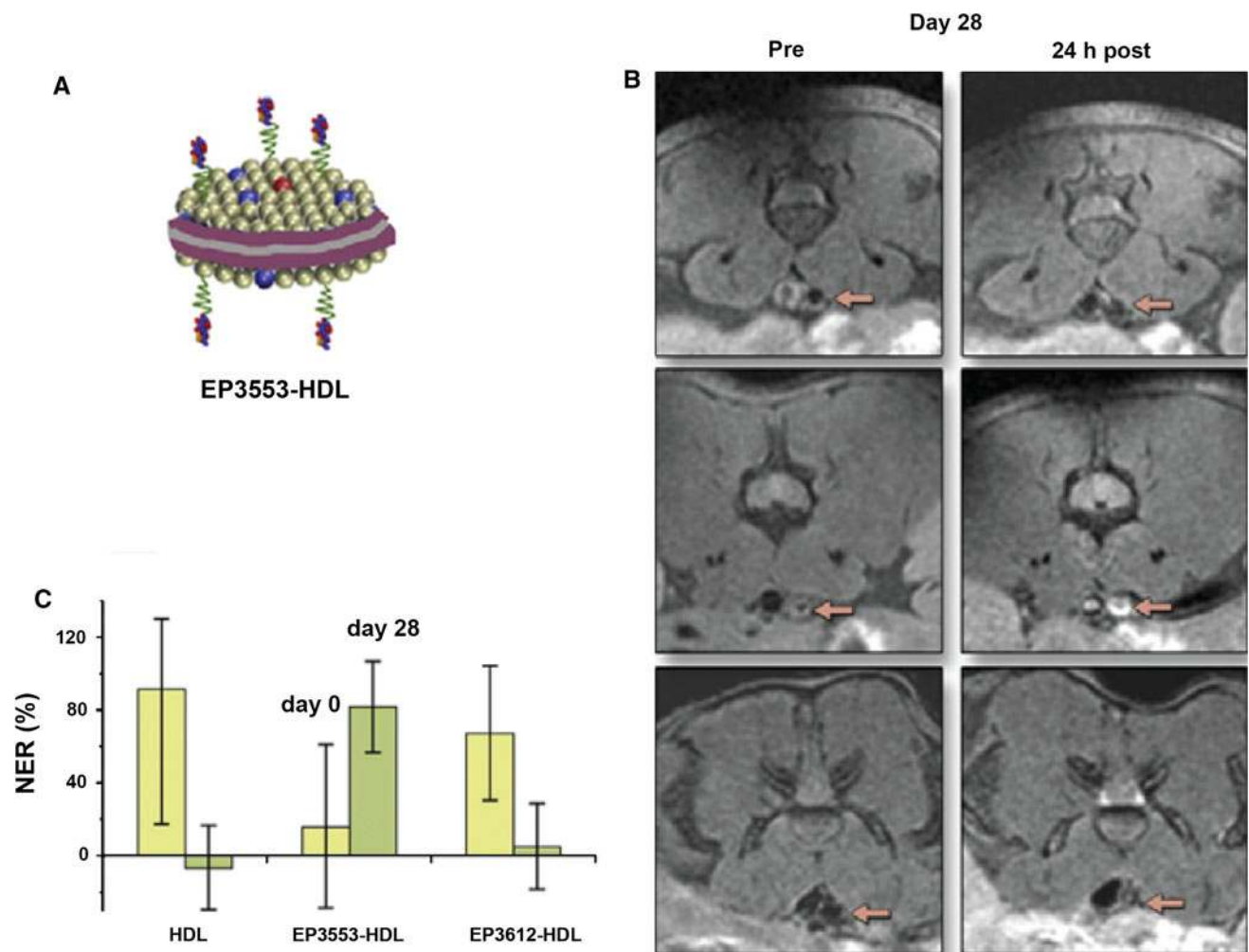
Fig. 6 MR imaging of atherosclerotic plaque regression with HDL and collagen-specific HDL nanoparticles. **a** Schematic drawing of high-density lipoprotein (HDL) nanoparticles functionalized with collagen-specific EP3553 peptides. **b** Representative transversal MR images of a Reversa mouse pre and 24 h post-injection of EP3553-HDL with enhanced signals in the regressing atherosclerotic plaques (*arrows*). **c** Normalized enhancement ratio (NER; plaque signal normalized to muscle) before (day 0) and after regression (day 28) resulting from injection of HDL, collagen-specific EP3553-HDL, or non-specific EP3612-HDL. Increased NER at day 28 for EP3553-HDL is an imaging readout for increased collagen content and decreased macrophage activity in the regressed plaques. *Reproduced from* [100••], *with permission*

Conclusions and Outlook

The last decade has witnessed an increased interest in the use of targeted nanoparticles as signal beacons for cardiovascular molecular imaging. The probes hold great promise for the facilitation of more specific patient diagnosis and treatment follow-up in the clinical management of atherosclerosis and myocardial infarction. Already a huge library of nanoparticles is available for specific imaging of various important hallmarks of CVD, including inflammation, dysfunctional endothelium, enzymatic activity, cell death, neovascularization, thrombosis, and extracellular matrix production or breakdown. Nevertheless, the field is eagerly awaiting clinical translation of some of these new disease-specific imaging technologies.

The use of the body's natural nanoparticles, such as HDL, for molecular imaging may accelerate such clinical translation. Generally, more knowledge is needed on the long-term fate of nanoparticles in the body and on the organ-clearance kinetics and pathways in view of possible toxicity.

The cardiovascular molecular imaging technology that we reviewed here can be employed for diagnosis or individualized evaluation of therapeutic interventions. Alternatively, nanoparticles can be equipped both with an imaging agent as well as with a therapeutic compound for a combined imaging and treatment protocol. This concept belongs to the broader field of theragnostics and personalized medicine [121, 122]. Treatment of myocardial infarction by stem cells to restore cardiac function and

improve myocardial perfusion has shown promising results in preclinical models. However, the rapid translation of stem cell treatment into the clinic has not yet yielded satisfactory results. Labeling of cells with nanoparticles for (cellular) molecular imaging of stem cell fate, migration, survival and engraftment gives better insights into therapeutic benefits and eventually may lead to improved treatment strategies [123]. Finally, regeneration of human cardiac tissue after myocardial infarction is actively explored in the field of cardiac tissue engineering, which aims to re-establish the structural and functional features of native myocardium, in a predictable way and on a long-term basis [124]. The development of cardiac tissue engineering is slowed down by the lack of suitable imaging technology for in vivo monitoring of implantation, cell proliferation, and tissue development. Here, nanoparticle-based molecular imaging could also prove to be of significant benefit.

Disclosure The authors declare no conflict of interest relevant to this article.

References

Papers of particular interest, published recently, have been highlighted as:
• Of importance,
•• Of major importance

1. World Health Organization. Global atlas on cardiovascular disease prevention and control; 2013. http://www.who.int/cardiovascular_diseases/en/. Accessed 4 Apr 2013.
2. Jaffer FA, Sosnovik DE, Nahrendorf M, Weissleder R. Molecular imaging of myocardial infarction. J Mol Cell Cardiol. 2006;41(6):921–33.
3. Sosnovik DE, Nahrendorf M, Weissleder R. Targeted imaging of myocardial damage. Nat Rev Cardiol. 2008;5:S63–70.
4. Leuschner F, Nahrendorf M. Molecular imaging of coronary atherosclerosis and myocardial infarction: considerations for the bench and perspectives for the clinic. Circ Res. 2011;108(5):593–606.
5. Majmudar MD, Nahrendorf M. Cardiovascular molecular imaging: the road ahead. J Nucl Med. 2012;53(5):673–6.
6. Dalager-Pedersen S, Ravn HB, Falk E. Atherosclerosis and acute coronary events. Am J Cardiol. 1998;82(10B):37T–40T.
7. Libby P. Inflammation in atherosclerosis. Nature. 2002;420(6917):868–74.
8. Falk E. Pathogenesis of atherosclerosis. J Am Coll Cardiol. 2006;47(8 Suppl):C7–12.
9. Blankesteijn WM, Creemers E, Lutgens E, Cleutjens JP, Daemen MJ, Smits JF. Dynamics of cardiac wound healing following myocardial infarction: observations in genetically altered mice. Acta Physiol Scand. 2001;173(1):75–82.
10. Frangogiannis NG. The mechanistic basis of infarct healing. Antioxid Redox Signal. 2006;8(11–12):1907–39.
11. Tawakol A, Migrino RQ, Hoffmann U, Abbara S, Houser S, Gewirtz H, et al. Noninvasive in vivo measurement of vascular inflammation with F-18 fluorodeoxyglucose positron emission tomography. J Nucl Cardiol. 2005;12(3):294–301.
12. Tawakol A, Migrino RQ, Bashian GG, Bedri S, Vermylen D, Cury RC, et al. In vivo 18F-fluorodeoxyglucose positron emission tomography imaging provides a noninvasive measure of carotid plaque inflammation in patients. J Am Coll Cardiol. 2006;48(9):1818–24.
13. Rudd JH, Fayad ZA. Imaging atherosclerotic plaque inflammation. Nat Clin Pract Cardiovasc Med. 2008;5(Suppl 2):S11–7.
14. Tahara N, Kai H, Ishibashi M, Nakaura H, Kaida H, Baba K, et al. Simvastatin attenuates plaque inflammation: evaluation by fluorodeoxyglucose positron emission tomography. J Am Coll Cardiol. 2006;48(9):1825–31.
15. Fujimura Y, Hwang PM, Trout Iii H, Kozloff L, Imaizumi M, Innis RB et al. Increased peripheral benzodiazepine receptors in arterial plaque of patients with atherosclerosis: an autoradiographic study with [(3)H]PK 11195. Atherosclerosis. 2008;201(1):108–11.
16. Balu N, Wang J, Dong L, Baluyot F, Chen H, Yuan C. Current techniques for MR imaging of atherosclerosis. Top Magn Reson Imaging. 2009;20(4):203–15.
17. Rosen BD, Litwin SE. The expanding role of computed tomography in the assessment of coronary artery disease and cardiac anatomy. Trends Cardiovasc Med. 2011;21(7):193–9.
18. Ruehm SG, Corot C, Vogt P, Kolb S, Debatin JF. Magnetic resonance imaging of atherosclerotic plaque with ultrasmall superparamagnetic particles of iron oxide in hyperlipidemic rabbits. Circulation. 2001;103(3):415–22.
19. Schmitz SA, Taupitz M, Wagner S, Wolf KJ, Beyersdorff D, Hamm B. Magnetic resonance imaging of atherosclerotic plaques using superparamagnetic iron oxide particles. J Magn Reson Imaging. 2001;14(4):355–61.
20. Kooi ME, Cappendijk VC, Cleutjens KB, Kessels AG, Kitslaar PJ, Borgers M, et al. Accumulation of ultrasmall superparamagnetic particles of iron oxide in human atherosclerotic plaques can be detected by in vivo magnetic resonance imaging. Circulation. 2003;107(19):2453–8.
21. Tang TY, Howarth SP, Miller SR, Graves MJ, Patterson AJ, U-King-Im JM, et al. The ATHEROMA (atorvastatin therapy: effects on reduction of macrophage activity) study. Evaluation using ultrasmall superparamagnetic iron oxide-enhanced magnetic resonance imaging in carotid disease. J Am Coll Cardiol. 2009;53(22):2039–50.
22. te Boekhorst BC, Bovens SM, Nederhoff MG, van de Kolk KW, Cramer MJ, van Oosterhout MF, et al. Negative MR contrast caused by USPIO uptake in lymph nodes may lead to false positive observations with in vivo visualization of murine atherosclerotic plaque. Atherosclerosis. 2010;210(1):122–9.
23. Kanno S, Wu YJ, Lee PC, Dodd SJ, Williams M, Griffith BP, et al. Macrophage accumulation associated with rat cardiac allograft rejection detected by magnetic resonance imaging with ultrasmall superparamagnetic iron oxide particles. Circulation. 2001;104(8):934–8.
24. Sosnovik DE, Nahrendorf M, Deliolanis N, Novikov M, Aikawa E, Josephson L, et al. Fluorescence tomography and magnetic resonance imaging of myocardial macrophage infiltration in infarcted myocardium in vivo. Circulation. 2007;115(11):1384–91.
25. Yang Y, Yang Y, Yanasak N, Schumacher A, Hu TC. Temporal and noninvasive monitoring of inflammatory-cell infiltration to myocardial infarction sites using micrometer-sized iron oxide particles. Magn Reson Med. 2010;63(1):33–40.
26. •• Alam SR, Shah AS, Richards J, Lang NN, Barnes G, Joshi N, et al. Ultrasmall superparamagnetic particles of iron oxide in patients with acute myocardial infarction: early clinical experience. Circ Cardiovasc Imaging. 2012;5(5):559–65. *Detection of*

inflammation in the myocardium of patients with acute myocardial infarction using MR imaging and ultrasmall superparamagnetic particles of iron oxide.

27. Naresh NK, Ben-Mordechai T, Leor J, Epstein FH. Molecular imaging of healing after myocardial infarction. Curr Cardiovasc Imaging Rep. 2011;4(1):63–76.

28. Naresh NK, Xu Y, Klibanov AL, Vandsburger MH, Meyer CH, Leor J, et al. Monocyte and/or macrophage infiltration of heart after myocardial infarction: MR imaging by using T1-shortening liposomes. Radiology. 2012;264(2):428–35.

29. Paulis LE, Geelen T, Kuhlmann MT, Coolen BF, Schafers M, Nicolay K, et al. Distribution of lipid-based nanoparticles to infarcted myocardium with potential application for MRI-monitored drug delivery. J Control Release. 2012;162(2):276–85.

30. • Geelen T, Paulis LE, Coolen BF, Nicolay K, Strijkers GJ. Passive targeting of lipid-based nanoparticles to mouse cardiac ischemia-reperfusion injury. Contrast Media Mol Imaging. 2013;8(2):117–26. *In this paper massive accumulation of non-targeted Gd-containing micelles and liposomes in a mouse model of ischemia-reperfusion myocardial injury by passive extravasation of the nanoparticles from the damaged vasculature was observed. Myocardial accumulation by passive extravasation hampers specific imaging with targeted nanoparticles, but opens new opportunities for delivering large payloads of therapeutics to the damage myocardium.*

31. Mulder WJ, Douma K, Koning GA, van Zandvoort MA, Lutgens E, Daemen MJ, et al. Liposome-enhanced MRI of neointimal lesions in the ApoE-KO mouse. Magn Reson Med. 2006;55(5):1170–4.

32. van Bochove GS, Paulis LE, Segers D, Mulder WJ, Krams R, Nicolay K, et al. Contrast enhancement by differently sized paramagnetic MRI contrast agents in mice with two phenotypes of atherosclerotic plaque. Contrast Media Mol Imaging. 2011;6(1):35–45.

33. Strijkers GJ, Hak S, Kok MB, Springer CS Jr, Nicolay K. Three-compartment T1 relaxation model for intracellular paramagnetic contrast agents. Magn Reson Med. 2009;61(5):1049–58.

34. Kok MB, Hak S, Mulder WJ, van der Schaft DW, Strijkers GJ, Nicolay K. Cellular compartmentalization of internalized paramagnetic liposomes strongly influences both T1 and T2 relaxivity. Magn Reson Med. 2009;61(5):1022–32.

35. Starmans LW, Kok MB, Sanders HM, Zhao Y, Donega Cde M, Meijerink A, et al. Influence of cell-internalization on relaxometric, optical and compositional properties of targeted paramagnetic quantum dot micelles. Contrast Media Mol Imaging. 2011;6(2):100–9.

36. Kok MB, Strijkers GJ, Nicolay K. Dynamic changes in 1H-MR relaxometric properties of cell-internalized paramagnetic liposomes, as studied over a five-day period. Contrast Media Mol Imaging. 2011;6(2):69–76.

37. Kok MB, de Vries A, Abdurrachim D, Prompers JJ, Grull H, Nicolay K, et al. Quantitative (1)H MRI, (19)F MRI, and (19)F MRS of cell-internalized perfluorocarbon paramagnetic nanoparticles. Contrast Media Mol Imaging. 2011;6(1):19–27.

38. Flögel U, Ding Z, Hardung H, Jander S, Reichmann G, Jacoby C, et al. In vivo monitoring of inflammation after cardiac and cerebral ischemia by fluorine magnetic resonance imaging. Circulation. 2008;118(2):140–8.

39. •• Temme S, Bönner F, Schrader J, Flögel U. 19F magnetic resonance imaging of endogenous macrophages in inflammation. WIREs Nanomed Nanobiotechnol. 2012;4(3):329–43. *This is an excellent review paper on the use of 19F MRI for imaging of macrophages in inflammation.*

40. Spahn DR. Blood substitutes. Crit Care. 1999;3(5):R91–2.

41. Maiseyeu A, Mihai G, Kampfrath T, Simonetti OP, Sen CK, Roy S, et al. Gadolinium-containing phosphatidylserine liposomes for molecular imaging of atherosclerosis. J Lipid Res. 2009;50(11):2157–63.

42. Geelen T, Yeo SY, Paulis LE, Coolen BF, Nicolay K, Strijkers GJ (eds). In vivo MR imaging of macrophages in cardiac ischemia/reperfusion injury with paramagnetic phosphatidylserine-containing liposomes. Proceedings of the 19th Annual Meeting ISMRM, Montreal; 2011.

43. Geelen T, Yeo SY, Paulis LE, Starmans LW, Nicolay K, Strijkers GJ. Internalization of paramagnetic phosphatidylserine-containing liposomes by macrophages. J Nanobiotechnol. 2012;10:37.

44. Amirbekian V, Lipinski MJ, Briley-Saebo KC, Amirbekian S, Aguinaldo JG, Weinreb DB, et al. Detecting and assessing macrophages in vivo to evaluate atherosclerosis noninvasively using molecular MRI. Proc Natl Acad Sci USA. 2007;104(3):961–6.

45. Mulder WJ, Strijkers GJ, Briley-Saboe KC, Frias JC, Aguinaldo JG, Vucic E, et al. Molecular imaging of macrophages in atherosclerotic plaques using bimodal PEG-micelles. Magn Reson Med. 2007;58(6):1164–70.

46. Briley-Saebo KC, Shaw PX, Mulder WJ, Choi SH, Vucic E, Aguinaldo JG, et al. Targeted molecular probes for imaging atherosclerotic lesions with magnetic resonance using antibodies that recognize oxidation-specific epitopes. Circulation. 2008;117(25):3206–15.

47. Lipinski MJ, Frias JC, Amirbekian V, Briley-Saebo KC, Mani V, Samber D, et al. Macrophage-specific lipid-based nanoparticles improve cardiac magnetic resonance detection and characterization of human atherosclerosis. JACC Cardiovasc Imaging. 2009;2(5):637–47.

48. te Boekhorst BC, Bovens SM, van de Kolk CW, Cramer MJ, Doevendans PA, ten Hove M, et al. The time window of MRI of murine atherosclerotic plaques after administration of CB2 receptor targeted micelles: inter-scan variability and relation between plaque signal intensity increase and gadolinium content of inversion recovery prepared versus non-prepared fast spin echo. NMR Biomed. 2010;23(8):939–51.

49. Kamat M, El-Boubbou K, Zhu DC, Lansdell T, Lu X, Li W, et al. Hyaluronic acid immobilized magnetic nanoparticles for active targeting and imaging of macrophages. Bioconjug Chem. 2010;21(11):2128–35.

50. Tsourkas A, Shinde-Patil VR, Kelly KA, Patel P, Wolley A, Allport JR, et al. In vivo imaging of activated endothelium using an anti-VCAM-1 magnetooptical probe. Bioconjug Chem. 2005;16(3):576–81.

51. Kelly KA, Allport JR, Tsourkas A, Shinde-Patil VR, Josephson L, Weissleder R. Detection of vascular adhesion molecule-1 expression using a novel multimodal nanoparticle. Circ Res. 2005;96(3):327–36.

52. Nahrendorf M, Jaffer FA, Kelly KA, Sosnovik DE, Aikawa E, Libby P, et al. Noninvasive vascular cell adhesion molecule-1 imaging identifies inflammatory activation of cells in atherosclerosis. Circulation. 2006;114(14):1504–11.

53. Jaffer FA, Nahrendorf M, Sosnovik D, Kelly KA, Aikawa E, Weissleder R. Cellular imaging of inflammation in atherosclerosis using magnetofluorescent nanomaterials. Mol Imaging. 2006;5(2):85–92.

54. van Bochove GS, Chatrou ML, Paulis LE, Grull H, Strijkers GJ, Nicolay K (eds). VCAM-1 targeted MRI for imaging of inflammation in mouse atherosclerosis using paramagnetic and superparamagnetic lipid-based contrast agents. Proceedings of the 18th Annual Meeting ISMRM, Stockholm; 2010.

55. McAteer MA, Sibson NR, von Zur Muhlen C, Schneider JE, Lowe AS, Warrick N, et al. In vivo magnetic resonance imaging of acute brain inflammation using microparticles of iron oxide. Nat Med. 2007;13(10):1253–8.

56. Jin AY, Tuor UI, Rushforth D, Filfil R, Kaur J, Ni F, et al. Magnetic resonance molecular imaging of post-stroke neuroinflammation with a P-selectin targeted iron oxide nanoparticle. Contrast Media Mol Imaging. 2009;4(6):305–11.

57. Hoyte LC, Brooks KJ, Nagel S, Akhtar A, Chen R, Mardiguian S, et al. Molecular magnetic resonance imaging of acute vascular cell adhesion molecule-1 expression in a mouse model of cerebral ischemia. J Cereb Blood Flow Metab. 2010;30(6): 1178–87.

58. Deddens LH, van Tilborg GA, van der Toorn A, van der Marel K, Paulis LE, van Bloois L, et al. MRI of ICAM-1 upregulation after stroke: the importance of choosing the appropriate target-specific particulate contrast agent. Mol Imaging Biol. 2013.

59. Akhtar AM, Schneider JE, Chapman SJ, Jefferson A, Digby JE, Mankia K, et al. In vivo quantification of VCAM-1 expression in renal ischemia reperfusion injury using non-invasive magnetic resonance molecular imaging. PLoS One. 2010;5(9):e12800.

60. Dall'Armellina E, Lygate CA, Mcateer M, Bohl S, Stork L-A, Neubauer S et al. (eds). *Ex vivo* and in vivo MR imaging of ischemia reperfusion injury in mouse hearts using microparticles of iron oxide targeting VCAM-1. Proceedings of the 18th Annual Meeting ISMRM, Stockholm; 10 Nov 2010.

61. Paulis LE, Jacobs I, van de Akker N, Geelen T, Molin D, Starmans LW, et al. Targeting of ICAM-1 on vascular endothelium under static and shear stress conditions using a liposomal Gd-based MRI contrast agent. J Nanobiotechnol. 2012; 10(1):25.

62. Lancelot E, Amirbekian V, Brigger I, Raynaud JS, Ballet S, David C, et al. Evaluation of matrix metalloproteinases in atherosclerosis using a novel noninvasive imaging approach. Arterioscler Thromb Vasc Biol. 2008;28(3):425–32.

63. Amirbekian V, Aguinaldo JG, Amirbekian S, Hyafil F, Vucic E, Sirol M, et al. Atherosclerosis and matrix metalloproteinases: experimental molecular MR imaging in vivo. Radiology. 2009;251(2):429–38.

64. Hyafil F, Vucic E, Cornily JC, Sharma R, Amirbekian V, Blackwell F, et al. Monitoring of arterial wall remodelling in atherosclerotic rabbits with a magnetic resonance imaging contrast agent binding to matrix metalloproteinases. Eur Heart J. 2011;32(12):1561–71.

65. te Boekhorst BC, Bovens SM, Hellings WE, van der Kraak PH, van de Kolk KW, Vink A, et al. Molecular MRI of murine atherosclerotic plaque targeting NGAL: a protein associated with unstable human plaque characteristics. Cardiovasc Res. 2011;89(3):680–8.

66. Querol M, Chen JW, Weissleder R, Bogdanov AJ. DTPA-bisamide-based MR sensor agents for peroxidase imaging. Org Lett. 2005;7(9):1719–22.

67. Querol M, Chen JW, Bogdanov AA. A paramagnetic contrast agent with myeloperoxidase-sensing properties. Org Biomol Chem. 2006;4(10):1887–95.

68. Ronald JA, Chen JW, Chen Y, Hamilton AM, Rodriguez E, Reynolds F, et al. Enzyme-sensitive magnetic resonance imaging targeting myeloperoxidase identifies active inflammation in experimental rabbit atherosclerotic plaques. Circulation. 2009;120(7):592–9.

69. • Nahrendorf M, Sosnovik D, Chen JW, Panizzi P, Figueiredo J-L, Aikawa E, et al. Activatable magnetic resonance imaging agent reports myeloperoxidase activity in healing infarcts and noninvasively detects the antiinflammatory effects of atorvastatin on ischemia-reperfusion injury. Circulation. 2008;117(9): 1153–60. *Application of a contrast agent that is activated by MPO activity in the injured myocardium. This approach allows noninvasive evaluation of the inflammatory response to ischemia and can be used to design new treatments aimed at modulating inflammation after myocardial infarction.*

70. Schellenberger EA, Sosnovik D, Weissleder R, Josephson L. Magneto/optical annexin V, a multimodal protein. Bioconjug Chem. 2004;15(5):1062–7.

71. Sosnovik DE, Schellenberger EA, Nahrendorf M, Novikov MS, Matsui T, Dai G, et al. Magnetic resonance imaging of cardiomyocyte apoptosis with a novel magneto-optical nanoparticle. Magn Reson Med. 2005;54(3):718–24.

72. van Tilborg GA, Mulder WJ, Chin PT, Storm G, Reutelingsperger CP, Nicolay K, et al. Annexin A5-conjugated quantum dots with a paramagnetic lipidic coating for the multimodal detection of apoptotic cells. Bioconjug Chem. 2006;17(4): 865–8.

73. van Tilborg GA, Mulder WJ, Deckers N, Storm G, Reutelingsperger CP, Strijkers GJ, et al. Annexin A5-functionalized bimodal lipid-based contrast agents for the detection of apoptosis. Bioconjug Chem. 2006;17(3):741–9.

74. van Tilborg GA, Geelen T, Duimel H, Bomans PH, Frederik PM, Sanders HM, et al. Internalization of annexin A5-functionalized iron oxide particles by apoptotic Jurkat cells. Contrast Media Mol Imaging. 2009;4(1):24–32.

75. Burtea C, Laurent S, Lancelot E, Ballet S, Murariu O, Rousseaux O, et al. Peptidic targeting of phosphatidylserine for the MRI detection of apoptosis in atherosclerotic plaques. Mol Pharm. 2009;6(6):1903–19.

76. Sosnovik DE, Garanger E, Aikawa E, Nahrendorf M, Figuiredo J-L, Dai G, et al. Molecular MRI of cardiomyocyte apoptosis with simultaneous delayed-enhancement MRI distinguishes apoptotic and necrotic myocytes in vivo: potential for mid-myocardial salvage in acute ischemia. Circ Cardiovasc Imaging. 2009;2(6):460–7.

77. van Tilborg GA, Vucic E, Strijkers GJ, Cormode DP, Mani V, Skajaa T, et al. Annexin A5-functionalized bimodal nanoparticles for MRI and fluorescence imaging of atherosclerotic plaques. Bioconjug Chem. 2010;21(10):1794–803.

78. Chen HH, Josephson L, Sosnovik DE. Imaging of apoptosis in the heart with nanoparticle technology. WIREs Nanomed Nanobiotechnol. 2011;3:86–99.

79. Garanger E, Hilderbrand SA, Blois JT, Sosnovik DE, Weissleder R, Josephson L. A DNA-binding Gd chelate for the detection of cell death by MRI. Chem Commun. 2009;7(29):4444–6.

80. Huang S, Chen HH, Yuan H, Dai G, Schuhle DT, Mekkaoui C, et al. Molecular MRI of acute necrosis with a novel DNA-binding gadolinium chelate: kinetics of cell death and clearance in infarcted myocardium. Circ Cardiovasc Imaging. 2011;4(6): 729–37. doi:10.1161/circimaging.111.966374.

81. Winter PM, Morawski AM, Caruthers SD, Fuhrhop RW, Zhang H, Williams TA, et al. Molecular imaging of angiogenesis in early-stage atherosclerosis with alpha(v)beta3-integrin-targeted nanoparticles. Circulation. 2003;108(18):2270–4.

82. Winter PM, Neubauer AM, Caruthers SD, Harris TD, Robertson JD, Williams TA, et al. Endothelial alpha(v)beta3 integrin-targeted fumagillin nanoparticles inhibit angiogenesis in atherosclerosis. Arterioscler Thromb Vasc Biol. 2006;26(9):2103–9.

83. Wickline SA, Neubauer AM, Winter PM, Caruthers SD, Lanza GM. Molecular imaging and therapy of atherosclerosis with targeted nanoparticles. J Magn Reson Imaging. 2007;25(4): 667–80.

84. Sirol M, Moreno PR, Purushothaman KR, Vucic E, Amirbekian V, Weinmann HJ, et al. Increased neovascularization in advanced lipid-rich atherosclerotic lesions detected by gadofluorine-M-enhanced MRI: implications for plaque vulnerability. Circ Cardiovasc Imaging. 2009;2(5):391–6.

85. Lanza GM, Winter PM, Caruthers SD, Hughes MS, Hu G, Schmieder AH, et al. Theragnostics for tumor and plaque angiogenesis with perfluorocarbon nanoemulsions. Angiogenesis. 2010;13(2):189–202.

86. Cai K, Caruthers SD, Huang W, Williams TA, Zhang H, Wickline SA, et al. MR molecular imaging of aortic angiogenesis. JACC Cardiovasc Imaging. 2010;3(8):824–32.

87. Lanza GM, Lorenz CH, Fischer SE, Scott MJ, Cacheris WP, Kaufmann RJ, et al. Enhanced detection of thrombi with a novel fibrin-targeted magnetic resonance imaging agent. Acad Radiol. 1998;5(Suppl 1):S173–6 (discussion S83–S84).

88. Johansson LO, Bjornerud A, Ahlstrom HK, Ladd DL, Fujii DK. A targeted contrast agent for magnetic resonance imaging of thrombus: implications of spatial resolution. J Magn Reson Imaging. 2001;13(4):615–8.

89. Marsh JN, Senpan A, Hu G, Scott MJ, Gaffney PJ, Wickline SA, et al. Fibrin-targeted perfluorocarbon nanoparticles for targeted thrombolysis. Nanomedicine (Lond). 2007;2(4):533–43.

90. Spuentrup E, Botnar RM, Wiethoff AJ, Ibrahim T, Kelle S, Katoh M, et al. MR imaging of thrombi using EP-2104R, a fibrin-specific contrast agent: initial results in patients. Eur Radiol. 2008;18(9):1995–2005.

91. von zur Muhlen C, von Elverfeldt D, Moeller JA, Choudhury RP, Paul D, Hagemeyer CE, et al. Magnetic resonance imaging contrast agent targeted toward activated platelets allows in vivo detection of thrombosis and monitoring of thrombolysis. Circulation. 2008;118(3):258–67.

92. Pan D, Senpan A, Caruthers SD, Williams TA, Scott MJ, Gaffney PJ, et al. Sensitive and efficient detection of thrombus with fibrin-specific manganese nanocolloids. Chem Commun (Camb). 2009;22:3234–6.

93. Katoh M, Haage P, Wiethoff AJ, Gunther RW, Bucker A, Tacke J, et al. Molecular magnetic resonance imaging of deep vein thrombosis using a fibrin-targeted contrast agent: a feasibility study. Invest Radiol. 2009;44(3):146–50.

94. Jansen CH, Perera D, Makowski MR, Wiethoff AJ, Phinikaridou A, Razavi RM, et al. Detection of intracoronary thrombus by magnetic resonance imaging in patients with acute myocardial infarction. Circulation. 2011;124(4):416–24.

95. Makowski MR, Forbes SC, Blume U, Warley A, Jansen CH, Schuster A, et al. In vivo assessment of intraplaque and endothelial fibrin in ApoE(−/−) mice by molecular MRI. Atherosclerosis. 2012;222(1):43–9.

96. Spuentrup E, Ruhl KM, Botnar RM, Wiethoff AJ, Buhl A, Jacques V, et al. Molecular magnetic resonance imaging of myocardial perfusion with EP-3600, a collagen-specific contrast agent: initial feasibility study in a swine model. Circulation. 2009;119(13):1768–75.

97. von Bary C, Makowski M, Preissel A, Keithahn A, Warley A, Spuentrup E, et al. MRI of coronary wall remodeling in a swine model of coronary injury using an elastin-binding contrast agent. Circ Cardiovasc Imaging. 2011;4(2):147–55.

98. Makowski MR, Wiethoff AJ, Blume U, Cuello F, Warley A, Jansen CH, et al. Assessment of atherosclerotic plaque burden with an elastin-specific magnetic resonance contrast agent. Nat Med. 2011;17(3):383–8.

99. Makowski MR, Preissel A, von Bary C, Warley A, Schachoff S, Keithan A, et al. Three-dimensional imaging of the aortic vessel wall using an elastin-specific magnetic resonance contrast agent. Invest Radiol. 2012;47(7):438–44.

100. •• Chen W, Cormode DP, Vengrenyuk Y, Herranz B, Feig JE, Klink A, et al. Collagen-specific peptide conjugated HDL nanoparticles as MRI contrast agent to evaluate compositional changes in atherosclerotic plaque regression. JACC Cardiovasc Imaging. 2013;6(3):373–84. *This study demonstrates that HDL nanoparticles can be used for in vivo MR imaging of macrophages and collagen in atherosclerotic plaque and changes therein upon plaque regression.*

101. Sanders HM, Strijkers GJ, Mulder WJ, Huinink HP, Erich SJ, Adan OC, et al. Morphology, binding behavior and MR-

102. Sanders HM, Iafisco M, Pouget EM, Bomans PH, Nudelman F, Falini G, et al. The binding of CNA35 contrast agents to collagen fibrils. Chem Commun (Camb). 2011;47(5):1503–5.

103. Klink A, Heynens J, Herranz B, Lobatto ME, Arias T, Sanders HM, et al. In vivo characterization of a new abdominal aortic aneurysm mouse model with conventional and molecular magnetic resonance imaging. J Am Coll Cardiol. 2011;58(24):2522–30.

104. van Bochove GS, Sanders HMHF, de Smet M, Keizer HM, Mulder WJM, Krams R, et al. Molecular MR imaging of collagen in mouse atherosclerosis by using paramagnetic CNA35 micelles. Eur J Inorg Chem. 2012;2012(12):2115–25.

105. Holgate ST. Exposure, uptake, distribution and toxicity of nanomaterials in humans. J Biomed Nanotechnol. 2010;6(1):1–19.

106. Nystrom AM, Fadeel B. Safety assessment of nanomaterials: implications for nanomedicine. J Control Release. 2012;161(2):403–8.

107. Huh YM, Lee ES, Lee JH, Jun YW, Kim PH, Yun CO, et al. Hybrid nanoparticles for magnetic resonance imaging of target-specific viral gene delivery. Adv Mater. 2007;19(20):3109–12.

108. Geninatti Crich S, Cutrin JC, Lanzardo S, Conti L, Kalman FK, Szabo I, et al. Mn-loaded apoferritin: a highly sensitive MRI imaging probe for the detection and characterization of hepatocarcinoma lesions in a transgenic mouse model. Contrast Media Mol Imaging. 2012;7(3):281–8.

109. Szabo I, Crich SG, Alberti D, Kalman FK, Aime S. Mn loaded apoferritin as an MRI sensor of melanin formation in melanoma cells. Chem Commun (Camb). 2012;48(18):2436–8.

110. Aime S, Frullano L, Geninatti Crich S. Compartmentalization of a gadolinium complex in the apoferritin cavity: a route to obtain high relaxivity contrast agents for magnetic resonance imaging. Angew Chem Int Ed Engl. 2002;41(6):1017–9.

111. Zheng G, Chen J, Li H, Glickson JD. Rerouting lipoprotein nanoparticles to selected alternate receptors for the targeted delivery of cancer diagnostic and therapeutic agents. Proc Natl Acad Sci USA. 2005;102(49):17757–62.

112. Navab M, Reddy ST, Van Lenten BJ, Fogelman AM. HDL and cardiovascular disease: atherogenic and atheroprotective mechanisms. Nat Rev Cardiol. 2011;8(4):222–32.

113. Cormode DP, Skajaa T, van Schooneveld MM, Koole R, Jarzyna P, Lobatto ME, et al. Nanocrystal core high-density lipoproteins: a multimodality contrast agent platform. Nano Lett. 2008;8(11):3715–23.

114. Nissen SE, Tsunoda T, Tuzcu EM, Schoenhagen P, Cooper CJ, Yasin M, et al. Effect of recombinant ApoA-I Milano on coronary atherosclerosis in patients with acute coronary syndromes: a randomized controlled trial. JAMA, J Am Med Assoc. 2003;290(17):2292–300.

115. Frias JC, Williams KJ, Fisher EA, Fayad ZA. Recombinant HDL-like nanoparticles: a specific contrast agent for MRI of atherosclerotic plaques. J Am Chem Soc. 2004;126(50):16316–7.

116. Cormode DP, Mulder WJM, Fisher EA, Fayad ZA. Modified lipoproteins as contrast agents for molecular imaging. Future Lipidol. 2007;2(6):587–90.

117. Cormode DP, Briley-Saebo KC, Mulder WJ, Aguinaldo JG, Barazza A, Ma Y, et al. An ApoA-I mimetic peptide high-density-lipoprotein-based MRI contrast agent for atherosclerotic plaque composition detection. Small. 2008;4(9):1437–44.

118. Skajaa T, Zhao Y, van den Heuvel DJ, Gerritsen HC, Cormode DP, Koole R, et al. Quantum Dot and Cy5.5 labeled nanoparticles to investigate lipoprotein biointeractions via forster resonance energy transfer. Nano Lett. 2010.

119. •• Cormode DP, Roessl E, Thran A, Skajaa T, Gordon RE, Schlomka JP, et al. Atherosclerotic plaque composition: analysis with multicolor CT and targeted gold nanoparticles. Radiology. 2010;256(3):774–82. *Spectral CT imaging using Au-HDL contrast agent can be used to detect macrophages in atherosclerosis, while imaging soft tissue, the vasculature and calcified tissues at the same time.*

120. Feig JE, Parathath S, Rong JX, Mick SL, Vengrenyuk Y, Grauer L, et al. Reversal of hyperlipidemia with a genetic switch favorably affects the content and inflammatory state of macrophages in atherosclerotic plaques. Circulation. 2011;123(9): 989–98.

121. Ginsburg GS, McCarthy JJ. Personalized medicine: revolutionizing drug discovery and patient care. Trends Biotechnol. 2001;19(12):491–6.

122. Ozdemir V, Williams-Jones B, Glatt SJ, Tsuang MT, Lohr JB, Reist C. Shifting emphasis from pharmacogenomics to theragnostics. Nat Biotechnol. 2006;24(8):942–6.

123. Fu Y, Azene N, Xu Y, Kraitchman DL. Tracking stem cells for cardiovascular applications in vivo: focus on imaging techniques. Imaging Med. 2011;3(4):473–86.

124. Vunjak-Novakovic G, Lui KO, Tandon N, Chien KR. Bioengineering heart muscle: a paradigm for regenerative medicine. Annu Rev Biomed Eng. 2011;13:245–67.